Pergamon

PII: S0301-9322(96)00060-2

Int. J. Multiphase Flow Vol. 23, No. 2, pp. 249–262, 1997

0301-9322/97 $17.00 + 0.00

STRUCTURE OF TURBULENT ROUND BUBBLING JET GENERATED BY PREMIXED GAS AND LIQUID INJECTION

M. IGUCHI[1]†, K. OKITA[2], T. NAKATANI[3] and N. KASAI[4]

[1]Department of Materials Science and Processing, Faculty of Engineering, Osaka University, 2-1 Yamada-oka, Suita, Osaka, 565 Japan
[2]Faculty of Engineering, Osaka University, 2-1 Yamada-oka, Suita, Osaka, 565 Japan
[3]Graduate School, Osaka University, 2-1 Yamada-oka, Suita, Osaka, 565 Japan
[4]Kashima Works, Sumitomo Metal Industries Ltd, Hikari, Kashima, Ibaraki, 314 Japan

(Received 14 January 1996)

Abstract—An air–water mixture was injected into a cylindrical water bath through a single-hole bottom nozzle to generate a vertical turbulent bubbling jet. A parameter called jet volume fraction, defined as the ratio of the air flow rate to the total flow rate of air and water, was introduced to specify the bubbling jet. The jet volume fraction was raised from zero to approximately 0.5 in order to study the effects of bubble concentration on the mean flow and turbulence characteristics in the water phase. Bubble diameters were roughly 2 mm and almost independent of the jet volume fraction. Water velocity measurements were made using a two-channel laser Doppler velocimeter. The effect of the jet volume fraction on the axial mean velocity of water was relatively weak, whereas the turbulence characteristics were significantly modulated. Turbulence production was enhanced with an increase in the jet volume fraction. The skewness and flatness factors, however, were not influenced by bubbles and agreed well with their respective values for single-phase free jets. Simplified methods of correlating the axial mean velocity, the root-mean-square values of the axial and radial turbulence components and Reynolds shear stress were proposed.

Key Words: gas–liquid two-phase flow, round bubbling jet, turbulence modulation, LDV, Reynolds shear stress, skewness factor, flatness factor

1. INTRODUCTION

In many engineering fields such as materials, chemical, mechanical and environmental engineering, gas injection techniques have been widely utilized for promoting chemical reactions, waste treatment, gas mixing and resolution, heat and mass transfer, and so on. Extensive model experiments have been carried out by many researchers by focusing on the flow field shown in figure 1(a) because gas injection through a bottom nozzle is most popular. As a result, much information on these subjects has been accumulated (Abdel Aal *et al.* 1966; Goosens and Smith 1975; Al Tawell and Landau 1977; McDougall 1978; Chesters *et al.* 1980; Milgram 1983; Bankovic *et al.* 1984; Durst *et al.* 1986; Sun and Faeth 1986a, b; Szekely *et al.* 1988; Gross and Kuhlman 1992; Sahai and Pierre 1992).

Compared with bubbling jets formed by the above-mentioned gas injection alone, investigations on bubbling jets generated due to premixed gas and liquid injections [see figure 1(b)] are rather limited (Sun and Faeth 1986a, b) though these bubbling jets have also been employed in many practical situations. In the present study we focused on this kind of turbulent round bubbling jet and carried out velocity measurements to reveal the modulation of the mean flow and turbulence characteristics in liquid phase due to the presence of bubbles.

The turbulence modulation in two-phase flows has drawn interest of many researchers for many years both from scientific and practical points of view. Although the size and concentration of particles or bubbles are considered main causes of the turbulence modulation, previous attention has been paid mainly to the effect of particle or bubble size on the turbulence modulation. Gore and Crowe (1989) examined previous experimental results of turbulence modulation in continuous

†Present address: Division of Materials Science and Engineering, Graduate School of Engineering, Hokkaido University, North 13, West 8, Kita-ku, Sapporo, 060, Japan.

phase due to particle or bubble addition (e.g. Serizawa *et al.* 1975a, b, c; Theofanous and Sallivan 1982; Tsuji *et al.* 1982, 1984; Marie and Lance 1983; Lance and Bataille 1991) and found that the turbulence intensity in the continuous phase was increased when the ratio of the particle diameter d_p to the integral length scale of turbulence in single-phase flow, l_e, exceeded a critical value of 0.1. When this ratio was less than 0.1, the tendency was reversed. As mentioned by Tsuji *et al.* (1994, 1995), the correlation by Gore and Crowe (1989) still bears a relatively large scatter of data points, and consequently, other parameters seem to be closely associated with the turbulence modulation.

Meanwhile, Hetsroni (1989) states that a low particle Reynolds number ($Re_p \lesssim 400$) tends to suppress the turbulence, whereas a high particle Reynolds number ($Re_p \gtrsim 400$) tends to enhance the turbulence. Here, $Re_p = \bar{u}_R d_p/\nu_f$, $\bar{u}_R[= \bar{u}_p - \bar{u}_f]$ is the relative velocity, $\bar{u}_p$ is the mean particle velocity, $\bar{u}_f$ is the mean velocity of surrounding fluid, and ν_f is the kinematic viscosity of fluid.

Concerning the effect of the concentration of particles on the turbulence modulation, some reports have been published recently. Tsuji *et al.* (1994, 1995) demonstrated from numerical simulations based on the DSMC (Direct Simulation Monte Carlo) method that the turbulence intensity in gas–solid flows in a vertical pipe varied strongly with respect to the concentration of particles, i.e. the number of particles per unit volume. Nihei and Nadaoka (1995) also investigated this effect numerically and reported that the turbulence modulation in gas–solid two-phase flows depended on the particle concentration in a complex manner.

On the other hand, there does not exist a consensus on the effect of the concentration of bubbles on the turbulence modulation in the continuous phase of gas–liquid flows. Our special attention, therefore, was paid to the effects of the concentration of bubbles on continuous (water) phase properties.

In order to change the concentration of bubbles in vertical bubbling jets by keeping the bubble diameter as constant as possible, we injected an air–water mixture through a single-hole bottom nozzle of a fixed inner diameter of 5 mm [see figure 1(b)]. Bubble diameters were kept almost constant of 2 mm regardless of the jet volume fraction defined by

$$\epsilon' = \frac{Q_G}{Q_G + Q_L} \qquad [1]$$

where Q_G and Q_L are the gas and water flow rates, respectively. This parameter was introduced to specify the degree of the concentration of bubbles in bubbling jets due to a reason described in a later section.

A bubbling jet similar to the present one was previously investigated by Sun and Faeth (1986a, b), who also used an aqueous system and carried out mean velocity and turbulence measurements with a laser Doppler velocimeter (LDV) for very dilute bubbling jets. The distribution of bubbles in the bubbling jet and bubble sizes were also measured using flash photography. Bubbles were roughly 1 mm in diameter. The jet volume fraction ranged from 0 [see figure 1(c)] to approximately 0.1. Sun and Faeth compared the experimental results with their own computational results based on three types of numerical analyses and found that the effects of

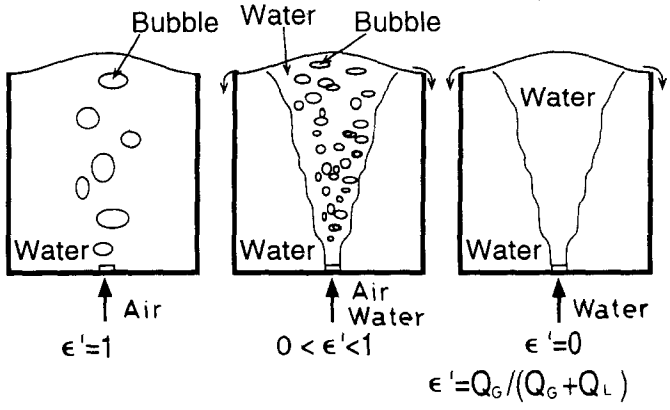

Figure 1. Schematic of bubbling jets in a water bath.

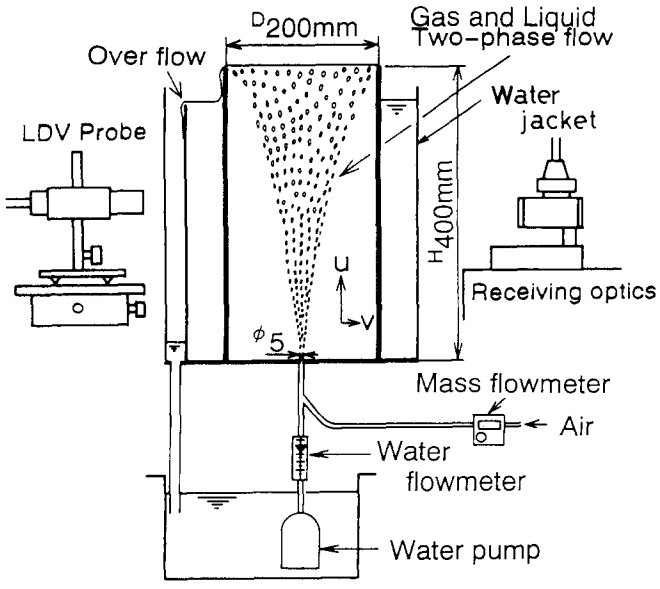

Figure 2. Experimental apparatus.

relative velocity, defined as the difference between the bubble rising velocity and the axial mean velocity of water, began to dominate the flow far from the nozzle, while effects of turbulent dispersion were important everywhere in the bubbling jet. However, the bubbling jets investigated by Sun and Faeth were very dilute ($\epsilon' < 0.1$), and hence, liquid phase properties were not strongly affected by interphase transport.

Accordingly, in order to evaluate the effect of the concentration of bubbles on liquid flow characteristics including turbulence modulation in bubbling jets generated by premixed gas and liquid injection in detail, we raised the jet volume fraction ϵ' from 0 to approximately 0.5 which was much higher than the maximum ϵ' value chosen by Sun and Faeth (1986a, b). Empirical correlations for the axial mean velocity, the root-mean-square (rms) values of the axial and radial turbulence components and the Reynolds shear stress were proposed for the first time as functions of ϵ'. Furthermore, higher turbulent correlations such as the skewness and flatness factors were obtained to specify the turbulence modulation in the bubbling jets in more detail.

2. EXPERIMENTAL APPARATUS AND PROCEDURE

Figure 2 shows a schematic diagram of the experimental apparatus. The transparent cylindrical vessel made of acrylic resin had an inner diameter of 200 mm and a height of 400 mm. Deionized water and air were premixed in a pipe connected upstream of a single-hole bottom nozzle of 5 mm in inner diameter d_n and injected into the deionized water bath through the nozzle. The water was circulated with a pump placed under the test vessel. The water flow rate was adjusted using a sluice valve and a rotameter. The air was supplied into the pipe with a compressor, and its flow rate was controlled by a mass flowmeter. A water jacket was used around the cylindrical vessel to avoid the effect of refraction on the measurements of bubble and liquid flow characteristics.

The origin of the cylindrical coordinate system was placed on the center of the nozzle exit. The axial (vertical) and radial (horizontal) coordinates were represented by z and r, respectively. The corresponding water velocity components were designated by u and v. Water velocity measurements were made using a two-channel laser Doppler velocimeter. Laser beams were frequently intercepted by bubbles especially near the nozzle exit, and hence, the data rate decreased to a very low level there. In addition, output signals of the LDV included bubble velocity signals. The number of bubble velocity signals became comparable to the number of water velocity signals near the nozzle exit as the jet volume fraction was raised.

We proposed previously a method of discriminating water velocity signals and bubble velocity signals using a two-channel LDV and a single-needle electroresistivity probe (Iguchi *et al.* 1994).

This method was not suitable for the present case because bubbles were so small that most of them could not be detected by the electroresistivity probe. Consequently, getting reliable water velocity data near the nozzle exit became difficult as ϵ' increased. On the other hand, in an axial region far from the nozzle exit, the number of bubble velocity signals was very small compared with that of water velocity signals, and reliable water velocity measurements were possible. The uncertainty of the present LDV measurements was estimated to be $\pm 3\%$.

Bubble diameters were determined by viewing photographs and the mean bubble diameter $\bar{d}_B$ was determined by averaging the measured bubble diameters. The mean bubble rising velocity $\bar{u}_B$ was obtained by measuring the vertical displacement of bubbles in photographs taken for a prescribed exposure time. The uncertainty of $\bar{d}_B$ and $\bar{u}_B$ measurements was estimated to be $\pm 3\%$. Other bubble characteristics such as void fraction and bubble frequency could not be precisely obtained because bubbles were too small to be detected by a two-needle electroresistivity probe (Iguchi *et al.* 1995a). Accordingly the quantitative evaluation of the bubble concentration was not possible at the present stage, and we decided to use the jet volume fraction ϵ' as a measure for describing the bubble concentration.

3. EXPERIMENTAL RESULTS AND DISCUSSION

3.1. Mean bubble diameter and mean relative velocity

Figure 3 shows rising bubbles taken by a camera for the jet volume fraction of $\epsilon' = 0.49$ ($Q_G = 40\ \text{cm}^3/\text{s}$, $Q_L = 42\ \text{cm}^3/\text{s}$). Bubble diameters were roughly 2 mm and almost independent of ϵ', as shown in figure 4. A gradual increase in the bubble diameter $\bar{d}_B$ with respect to the axial distance z was caused by the coalescence of bubbles. In general, the phenomenon of bubble coalescence depends on bubble size, contamination, turbulence, liquid properties, small vibration of experimental facilities and so on. It is considered that the coalescence of bubbles observed here is not inherent of the present experimental equipment because the contamination and the vibration were prevented satisfactorily. A change in the bubble volume due to a decrease in the hydrostatic pressure was negligibly small under the present experimental conditions. Almost the same results were obtained for $Q_G = 83\ \text{cm}^3/\text{s}$. The outer edge of the bubble dispersion region was hardly affected by ϵ'. This fact means that the bubble concentration in the bubbling jet increases almost linearly with respect to ϵ'. The mean relative velocity $\bar{u}_R$ was roughly 20 cm/s.

3.2. Centerline value $\bar{u}_{cl}$ and half-value radius b_u of the radial distribution of the axial mean velocity component $\bar{u}$

Figure 5 shows measured values of $\bar{u}_{cl}$ and b_u obtained under various experimental conditions where b_u denotes the distance from the centerline to the radial position at which $\bar{u}$ becomes half the centerline value $\bar{u}_{cl}$. Centerline quantities are designated by the subscript cl. Although the measured values are plotted in the axial region ranging from the nozzle exit to the vicinity of the bath surface, those for larger ϵ' values have considerable uncertainty near the nozzle exit ($z \lesssim 5$ cm for $Q_L = 42\ \text{cm}^3/\text{s}$ and $z \lesssim 7.5$ cm for $Q_L = 83\ \text{cm}^3/\text{s}$) from the reason mentioned earlier in section 2.

The effects of the jet volume fraction ϵ' on the centerline value $\bar{u}_{cl}$ and half-value radius b_u were relatively weak. In the case of a single bubble, the bubble rising velocity reaches a terminal velocity, and hence, the liquid velocity also approaches a terminal value. It is not clear whether the present $\bar{u}_{cl}$ value approaches a terminal velocity or not because the bath is not deep enough.

3.3. Rms values of the axial and radial turbulence components on the centerline

Measured rms values of the axial and radial turbulence components on the centerline, $u'_{rms,cl}$ and $v'_{rms,cl}$, for $Q_L = 42\ \text{cm}^3/\text{s}$ are shown in figure 6. Compared with the $\bar{u}_{cl}$ and b_u values, these values are very sensitive to the gas flow rate Q_G, and hence, to the jet volume fraction ϵ'. This fact implies that bubbles affect turbulence production significantly.

According to Wygnanski and Fiedler (1969), the integral length scale, l_e in single-phase free jets is described by $l_e = 0.039z$. Under the present experimental conditions $\bar{d}_B \approx 2$ mm and l_e ranges from 3.9 to 7.8 mm, and accordingly $\bar{d}_B/l_e$ falls approximately between 0.25 and 0.51. On the other hand, Gibson (1963) derived a relation of $l_e = 0.081z$. This relation gives the largest l_e value among

existing empirical relations for l_e. Even in this case, the present $\bar{d}_B$ value is larger than 0.1 l_e. From this result and the data in figure 6, it became evident that the relation proposed by Gore and Crowe (1989) for the particle diameter and turbulence modulation is valid under the present experimental conditions. A bubble Reynolds number Re_B ($=\bar{u}_R\bar{d}_B/\nu_L$, $\bar{u}_R = \bar{u}_B - \bar{u}$: relative velocity, ν_L: kinematic viscosity of liquid) is estimated to be larger than approximately 400, implying that Hetsroni's prediction is also valid.

It can be concluded from a comparison between figures 5 and 6 that the energy introduced into a bath by the inertia force of injected gas and by the buoyancy of bubbles generated in the bath due to disintegration of the injected gas is mainly consumed to enhance turbulence production without affecting mean flow motions in the liquid phase significantly.

3.4. Derivation of an empirical correlation for the axial mean velocity $\bar{u}$

Although some numerical simulation methods have been developed, for example, by Sun and Faeth (1986a, b), it is useful from a practical point of view to derive a simple empirical correlation capable of predicting the axial mean velocity $\bar{u}$.

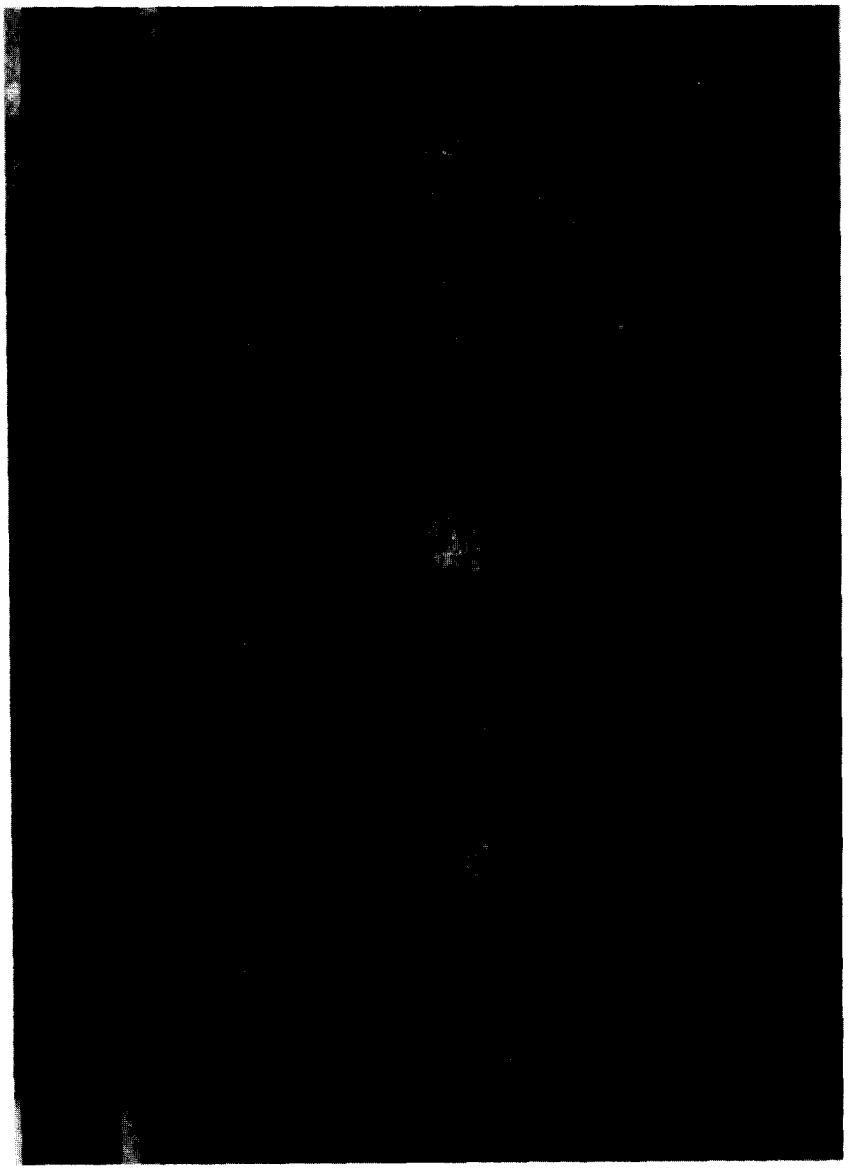

Figure 3. Rising bubbles taken by a camera for $\epsilon' = 0.49$ ($Q_G = 40\ cm^3/s$, $Q_L = 42\ cm^3/s$).

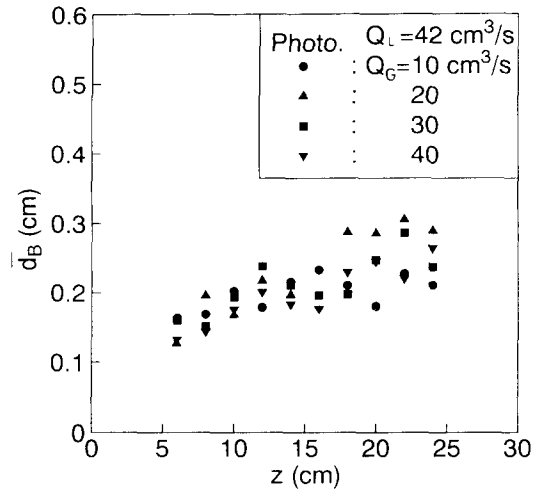

Figure 4. Axial distributions of bubble diameter for $Q_L = 42$ cm³/s.

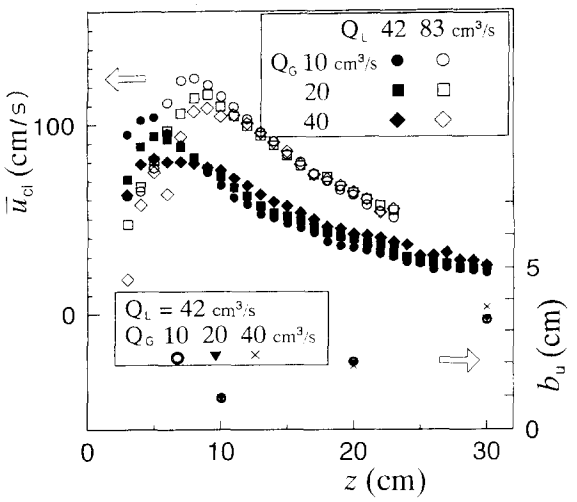

Figure 5. Axial distributions of the centerline value and half-value radius of axial mean velocity $\bar{u}$.

Reichardt (1943) proposed the following correlation for the axial mean velocity $\bar{u}$ in the far field in single-phase free jets

$$\frac{\bar{u}}{\bar{u}_0} = \frac{1}{2C\left(\frac{z}{d_n}\right)} \exp\left[\frac{-r^2}{2C^2z^2}\right] \qquad [2]$$

where $\bar{u}_0$ is the velocity at the nozzle exit, C is the fitting parameter, r is the radial distance, z is the axial distance, and d_n is the inner diameter of the nozzle.

Popper *et al.* (1974) found that [2] is valid for dilute solid particle-laden air jets. Although there is no definite similarities between gas–liquid and gas–solid two-phase flows, for the sake of simplicity, we also choose [2] as a candidate for correlating the axial mean velocity of water in the bubbling jets because bubbles are almost spherical in shape under the present experimental conditions.

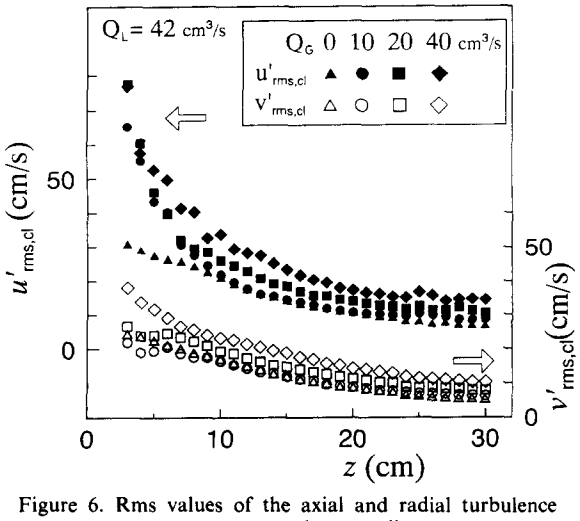

Figure 6. Rms values of the axial and radial turbulence components on the centerline.

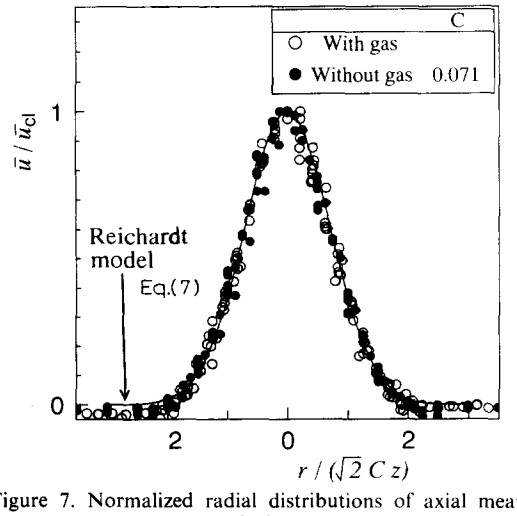

Figure 7. Normalized radial distributions of axial mean velocity.

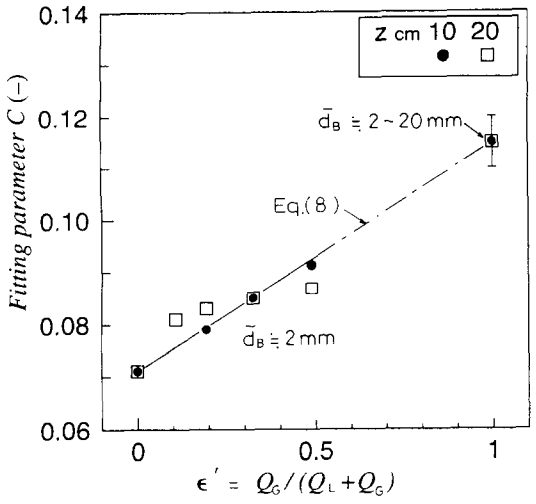

Figure 8. Relation between fitting parameter C and jet volume fraction ϵ'.

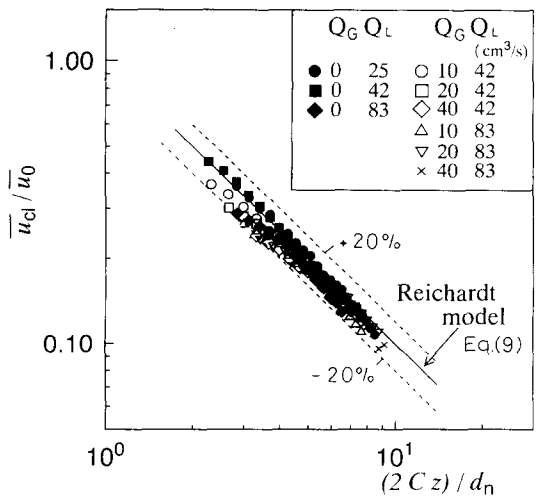

Figure 9. Comparison of the present model [9], with measured values of the centerline velocity.

Furthermore, we will use the following drift flux model developed by Zuber and Findlay (1965) to evaluate the exit water velocity $\bar{u}_0$

$$\bar{u}_0 = \frac{(1 - C_0\epsilon')j_T - \epsilon' V_{G_j}}{1 - \epsilon'} \quad [3]$$

where C_0 is the distribution parameter, j_T is the average volumetric flux density, and V_{G_j} is the drift velocity. Since the flow in the nozzle is regarded as the so-called bubbly flow under the present experimental conditions, the following expressions are employed

$$C_0 = 1.2 - 0.2\left(\frac{\rho_G}{\rho_L}\right)^{1/2} \quad [4]$$

$$j_T = \frac{Q_L + Q_G}{A} \quad [5]$$

$$V_{G_j} = \sqrt{2}\left(\frac{\sigma g(\rho_L - \rho_G)}{\rho_L^2}\right)^{1/4} \quad [6]$$

where ρ_L is the density of liquid, ρ_G is the density of gas, A $(=\pi d_n^2/4)$ is the cross-sectional area of the nozzle, and σ is the surface tension of liquid.

We determined the fitting parameter C by fitting measured $\bar{u}$ values to the following equation.

$$\frac{\bar{u}}{\bar{u}_{cl}} = \exp\left[-\frac{r^2}{2C^2z^2}\right]. \quad [7]$$

This equation was derived from [2]. Figure 7 demonstrates that measured $\bar{u}$ values for all runs are satisfactorily correlated by [7] where the measured value of $\bar{u}$ on the centerline was substituted for $\bar{u}_{cl}$.

The fitting parameter C thus obtained was shown in figure 8 as a function of the jet volume fraction ϵ'. Data for the gas injection alone ($\epsilon' = 1$) were included. The present measured values can be reasonably approximated by a solid line described by

$$C = 0.046\epsilon' + 0.071 \quad (0 \leqslant \epsilon' < 0.5). \quad [8]$$

It is interesting to note that the measured values for $\epsilon' = 1$ are also approximated by [8].

Comparison between nondimensionalized centerline values, $\bar{u}_{cl}/\bar{u}_0$, and the present model was given in figure 9. Measured values obtained near the nozzle exit are not included because of high measurement errors. All the measured values shown in figure 9 were approximated by the following equation, derived by substituting zero into r in [2], within a scatter of $\pm$ 20%

$$\frac{\bar{u}_{cl}}{\bar{u}_0} = \frac{1}{2C(z/d_n)}. \qquad [9]$$

The half-value radius b_u can be written as a function of the fitting parameter C and the axial distance z as follows:

$$b_u = \sqrt{2 \cdot \ln 2} Cz. \qquad [10]$$

The inner diameter of the single-hole nozzle was fixed in this study ($d_n = 5$ mm). If d_n changes, bubble diameters would change depending on d_n. The experimental results for $\epsilon' = 1$ suggest that the fitting parameter C is not sensitive to the bubble diameter $\bar{d}_B$ (2 mm $\lesssim \bar{d}_B \lesssim$ 20 mm) also for bubbling jets of $\epsilon' < 1$. Examination of the applicability of [8] to bubbling jets of different bubble diameters should be left for a future study.

It should be stressed that the radial distribution of $\bar{u}$ in bubbling jets for gas injection alone ($\epsilon' = 1$) can be approximated by [7] as well, but the centerline value $\bar{u}_{cl}$ cannot be correlated by [9] because $\bar{u}_0$ becomes infinite for $\epsilon' = 1$ and looses its physical meaning. Concerning an empirical correlation of $\bar{u}_{cl}$ in bubbling jets for $\epsilon' = 1$, see Iguchi *et al.* (1995b).

Figure 10 shows a comparison between the present model and measured $\bar{u}_{cl}/j_T$ values obtained by Sun and Faeth (1986a). Experimental conditions for the single-phase jet and three types of bubbling jets (cases I, II, III) are listed in table 1 in their original paper. A solid and a broken line denote computational results based on the LHF model and SSF and DSF model, where LHF,

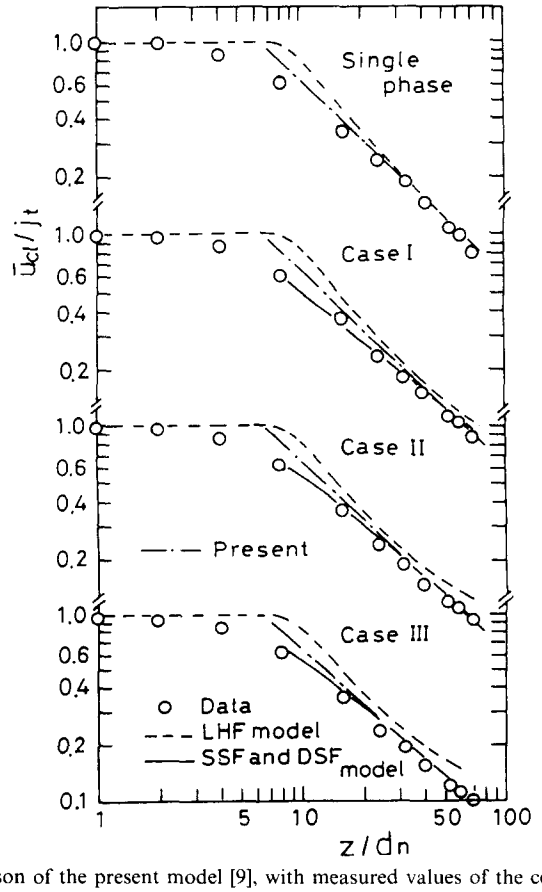

Figure 10. Comparison of the present model [9], with measured values of the centerline velocity by Sun and Faeth.

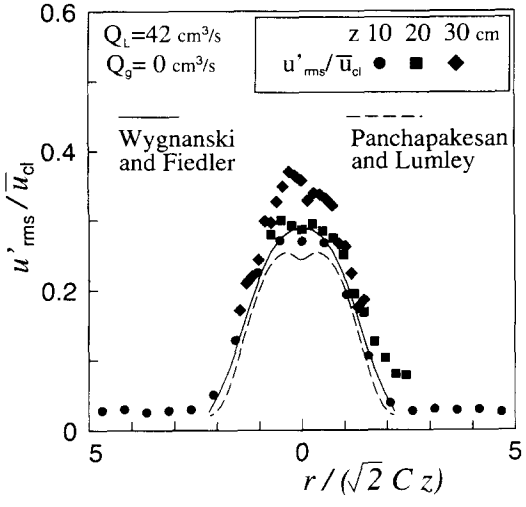

Figure 11. Radial distributions of the nondimensionalized rms values of axial turbulence component for water jet.

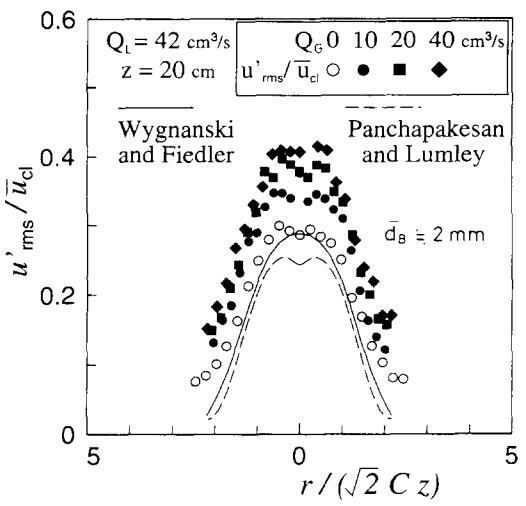

Figure 12. Radial distributions of the nondimensionalized rms values of axial turbulence component for bubbling jet.

SSF and DSF are the abbreviations of the "locally homogeneous flow", "stochastic separated flow", and "deterministic separated flow" analyses, respectively. Details of these methods should be referred to Sun and Faeth (1986a). In every case, the present model can predict the measured values in the axial region except the vicinity of the nozzle exit.

Although any evidence was not given here, measured radial distributions of the axial mean velocity in the four cases mentioned above were also reasonably predicted by the present model.

3.5. Radial distributions of the rms values of axial and radial turbulence components, u'_{rms} and v'_{rms}, and Reynolds shear stress, $\overline{u'v'}$

Measured values of u'_{rms} for single-phase jets were nondimensionalized by the centerline value of the axial mean velocity, $\bar{u}_{cl}$, and plotted against $r/(\sqrt{2}Cz)$ in figure 11. The water flow rate Q_L was 42 cm³/s and the axial measurement position was z = 10, 20, or 30 cm. A solid line and a broken line indicate the rms values for single-phase free jets measured by Wygnanski and Fiedler (1969) and Panchapakesan and Lumley (1993), respectively. The present measured values for z = 10 and 20 cm were in good agreement with the single-phase free jet curve in the radial region of $r/(\sqrt{2}Cz) \lesssim 1.5$. Outside this radial region, side wall effects emerged. The measured values for z = 30 cm became much larger than the single-phase free jet values because this axial measurement

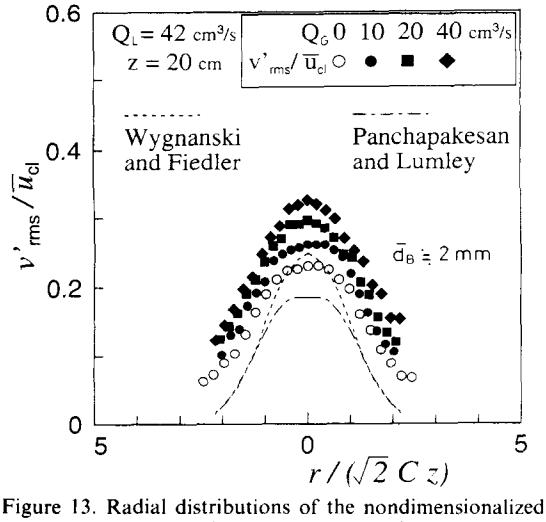

Figure 13. Radial distributions of the nondimensionalized rms value of radial turbulence component for bubbling jet.

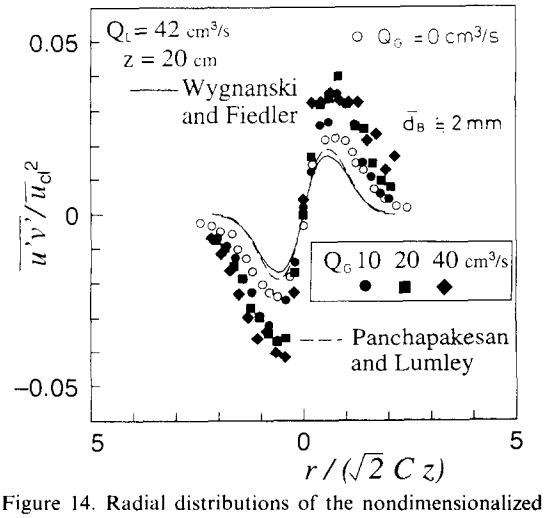

Figure 14. Radial distributions of the nondimensionalized Reynolds shear stress for bubbling jet.

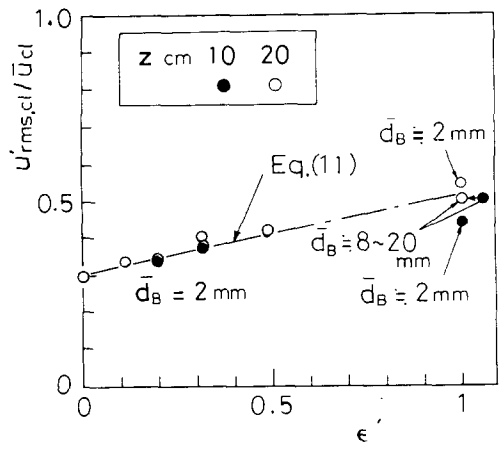

Figure 15. Relation between axial turbulence intensity on the centerline and jet volume fraction.

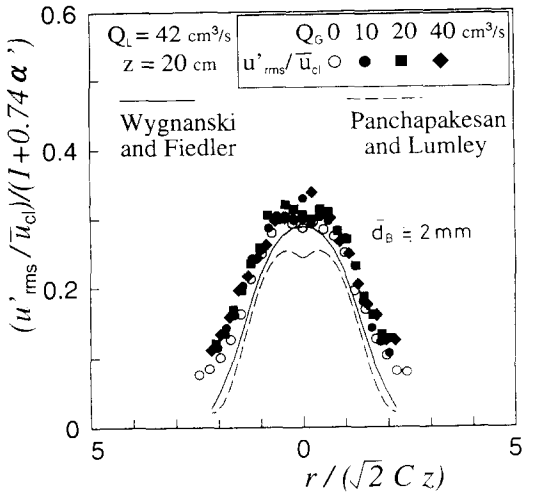

Figure 16. Relation between modified axial turbulence intensity and jet volume fraction.

position was influenced significantly by the side wall as well as the surface flow directed outward. In what follows, data for $z = 10$ and 20 cm, therefore, will be shown.

Bubbling jet data on $u'_{rms}/\bar{u}_{cl}$ were plotted in figure 12. As the gas flow rate increased, the measured $u'_{rms}/\bar{u}_{cl}$ values increased everywhere in the bubbling jet region of $r/(\sqrt{2}Cz) \lesssim 1.5$. Such turbulence intensity enhancement is attributable to additional turbulence production in the wake of bubbles (e.g. Iguchi *et al.* 1991, 1995a; Sheng and Iron 1992).

The same conclusion as above can be derived from the radial distributions of $v'_{rms}/\bar{u}_{cl}$, as shown in figure 13. Furthermore, measured values of the Reynolds shear stress divided by the square of the centerline velocity, $\overline{u'v'}/\bar{u}_{cl}^2$, increased with an increase in ϵ' (see figure 14).

The ratio of $u'_{rms,cl}/\bar{u}_{cl}$ for the bubbling jet to that for the single-phase jet, denoted by r_t, was determined as a function of the jet volume fraction ϵ'.

The $u'_{rms,cl}/\bar{u}_{cl}$ values thus obtained for $\bar{d}_B \approx 2$ mm can be correlated by the following empirical equation, as shown in figure 15.

$$\frac{u'_{rms,cl}}{\bar{u}_{cl}} = 0.31 r_t \qquad [11]$$

$$r_t = 1 + 0.74\epsilon' \quad (0 \leqslant \epsilon' < 0.5). \qquad [12]$$

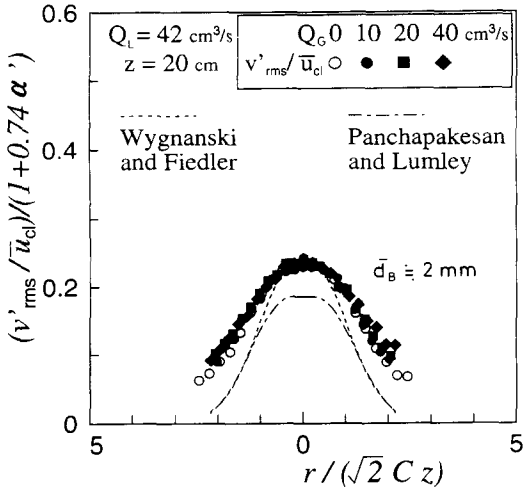

Figure 17. Relation between modified radial turbulence intensity and jet volume fraction.

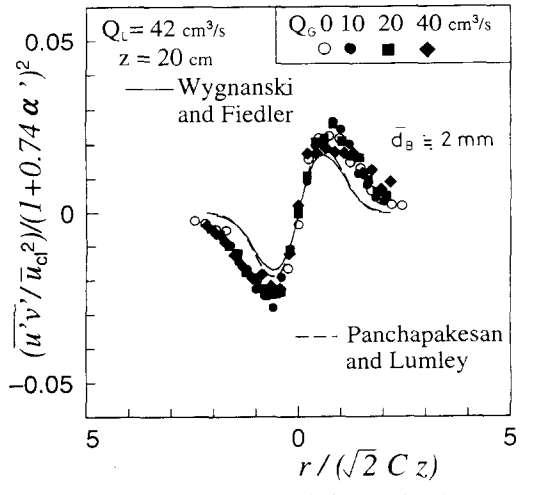

Figure 18. Relation between modified Reynolds shear stress and jet volume fraction.

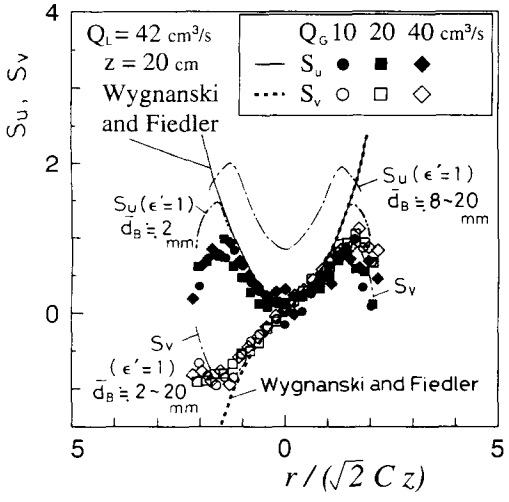

Figure 19. Radial distributions of skewness factors of axial and radial turbulence components, S_u and S_v.

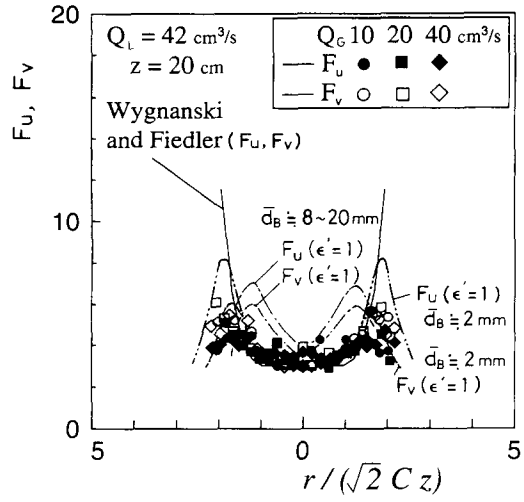

Figure 20. Radial distributions of flatness factors of axial and radial turbulence components, F_u and F_v.

Measured values of $u'_{rms}/\bar{u}_{cl}$, $v'_{rms}/\bar{u}_{cl}$, and $\overline{u'v'}/\bar{u}_{cl}^2$ were divided by r_t, r_t, and r_t^2, respectively, and replotted in figure 16–18. In each figure the measured values are well correlated by this method.

3.6. Skewness and flatness factors

The skewness and flatness factors, S and F, are two of measures characterizing probability distribution functions. No one has mentioned about higher turbulent correlations such as the skewness and flatness factors in turbulent bubbling jets generated by premixed gas and liquid injection. The definitions of these factors are given, for example, by Wygnanski and Fiedler (1969), Hinze (1975) and Hino (1977). If probability distribution functions obey Gaussian distributions, it follows that $S = 0$ and $F = 3$. Measured values of the skewness factors for the axial and radial turbulence components, denoted by S_u and S_v, are plotted in figure 19. A solid line and a broken line designate S_u and S_v values for single-phase jets obtained by Wygnanski and Fiedler (1969), respectively.

In the central part of the bubbling jet region, $r/(\sqrt{2}Cz) \lesssim 1.5$, the present measured values of S_u and S_v agreed with their respective values for the single-phase free jet. This fact means that rising bubbles of approximately 2 mm in diameter do not exert any influence on the shape of the probability distribution functions of the axial and radial turbulence components though the bubbles enhance turbulence production significantly.

For bubbling jets of $\epsilon' = 1$ and $\bar{d}_B \approx 8 \sim 20$ mm, S_u became much larger than the single-phase free jet value (Iguchi *et al.* 1995a), as can be seen in figure 19. Decreasing the bubble diameter for gas injection alone ($\epsilon' = 1$) was achieved by making use of a porous nozzle (Iguchi *et al.* 1996). Bubble diameters were decreased to approximately 2 mm. In this case, the distributions of S_u and S_v were almost the same as those obtained here for bubbling jets of $\epsilon' < 0.5$ and $\bar{d}_B \approx 2$ mm. Consequently, the jet volume fraction ϵ' hardly affect the skewness factors of the axial and radial turbulence components, whereas the bubble size does them strongly. This result seems to be closely associated with the scale of turbulence in the wake of bubbles.

Meanwhile, comparison of the present results with previous ones for gas injection alone indicates that the skewness factor of the radial turbulence component, S_v, is hardly affected by the size of bubbles for $r/(\sqrt{2}Cz) \lesssim 1.5$ and agreed with that for single-phase free jets.

The flatness factors for the axial and radial turbulence components, F_u and F_v, obtained here agreed with each other for $r/(\sqrt{2}Cz) \lesssim 1.5$ and almost followed the single-phase free jet curve obtained by Wygnanski and Fiedler (1969), as shown in figure 20. The flatness factors were also dependent on the bubble diameter.

4. CONCLUSIONS

Mean flow and turbulence characteristics in the liquid phase in turbulent round bubbling jets generated by injecting an air and water mixture into a water bath were measured using a two-channel laser Doppler velocimeter. The ratio of the bubble diameter $\bar{d}_B$ to the integral length scale of turbulence, l_e, in single-phase jets was larger than the critical value of 0.1 found by Gore and Crowe (1989) for the turbulence modulation. The jet volume fraction ϵ' was changed from zero to approximately 0.5 to study the modulation of the above characteristics. Bubble diameters were roughly 2 mm and almost independent of ϵ'. The bubble Reynolds number was greater than approximately 400. Main findings obtained in the central part of the bubbling jet, $r/(\sqrt{2Cz}) \lesssim 1.5$, are summarized as follows

(1) The effect of the jet volume fraction ϵ' on the axial (vertical) mean velocity $\bar{u}$ was relatively weak, whereas the rms values of the axial and radial turbulence components and the Reynolds shear stress were highly increased with an increase in ϵ'. Consequently, the energy introduced into the bath by the inertia force of injected gas and the buoyancy of bubbles generated in the bath due to disintegration of the injected gas is mainly consumed to generate turbulence.

(2) A comparison of the present experimental results of the skewness factor with previous ones for $\epsilon' = 1$ revealed that the skewness factor for the axial turbulence component, S_u, in the bubbling jet was hardly dependent on the jet volume fraction ϵ' but strongly dependent on the size of bubbles. As the mean bubble diameter increased, S_u increased and became much larger than the measured value for single-phase free jets. Under the present experimental conditions, however, S_u almost followed the single-phase free jet curve. This is because the mean bubble diameter $\bar{d}_B$ is small enough but larger than 0.1 l_e. The skewness factor for the radial turbulence component was not influenced by the size of bubbles.

Both the flatness factors for the axial and radial turbulence components, F_u and F_v, agreed with each other and yet followed single-phase free jet value. Accordingly the effects of ϵ' on F_u and F_v were negligible. These flatness factors were also influenced by the size of bubbles.

(3) The axial mean velocity of water, $\bar{u}$, was satisfactorily correlated by the Reichardt model. In the Reichardt model, the mean water velocity at the nozzle exit, $\bar{u}_0$, was evaluated from the drift flux model by assuming the bubbly flow in the nozzle. This prediction method was newly proposed in this study. The experimental results of $\bar{u}$ reported by Sun and Faeth were predicted by this method as well.

(4) A simplified method was proposed to correlate the rms values of the axial and radial turbulence components and the Reynolds shear stress as functions of the jet volume fraction ϵ'.

REFERENCES

Abdel-Aal, H. K., Stiles, G. B. and Holland, C. D. (1966) Formation of interfacial area at high rates of gas flow through submerged orifices. *AIChE J.* **12,** 174–180.

Al Tawell, A. M. and Landau, J. (1977) Turbulence modulation in two-phase jets. *Int. J. Multiphase Flow* **3,** 341–353.

Bankovic, A., Currie, I. G. and Martin, W. W. (1984) Laser–Doppler measurements of bubble plumes. *Phys. Fluids* **27,** 348–355.

Chesters, A. K., van Doorn, M. and Goossens, L. H. J. (1980) A general model of unconfined bubble plumes from an extended source. *Int. J. Multiphase Flow* **6,** 499–521.

Durst, F., Schonung, B., Selanger K. and Winter, M. (1986) Bubble driven liquid flows. *J. Fluid Mech.* **170,** 53–82.

Gibson, M. M. (1963) Spectra of turbulence in a round jet. *J. Fluid Mech.* **15,** 161–173.

Goossens, L. H. J. and Smith, J. M. (1975) The hydrodynamics of unconfined bubble columns for mixing lakes and reservoirs. *Chem. Eng. Tech.* **47,** 951.

Gore, R. A. and Crowe, C. T. (1989) Effect of particle size on modulating turbulent intensity. *Int. J. Multiphase Flow* **15,** 279–285.

Gross, R. W. and Kuhlman, J. M. (1992) Three-component velocity measurements in a turbulent recirculating bubble-driven liquid flow. *Int. J. Multiphase Flow* **18,** 413–421.

Hetsroni, G. (1989) Particle-turbulence interaction. *Int. J. Multiphase Flow* **15,** 735–746.

Hino, M. (1977) *Spectrum Analysis*, p. 107. Asakura Book Co. Ltd, New York.

Hinze J. O. (1975) *Turbulence*, 2nd edition. McGraw-Hill, New York.

Iguchi, M., Takeuchi, H. and Morita, Z. (1991) The flow fields in air–water vertical bubbling jets in a cylindrical vessel. *ISIJ Int.* **32,** 246–253.

Iguchi, M., Kondoh, T. and Uemura, T. (1994) Simultaneous measurement of liquid and bubble velocities in a cylindrical bath subject to centric bottom gas injection. *Int. J. Multiphase Flow* **20,** 753–762.

Iguchi, M., Ueda, H. and Uemura, T. (1995a) Bubble and liquid flow characteristics in a vertical bubbling jet. *Int. J. Multiphase Flow* **21,** 861–873.

Iguchi, M., Kondoh, T., Morita, Z., Nakajima, K., Hanazaki, H., Uemura, T. and Yamamoto, F. (1995b) Velocity and turbulence measurements in a cylindrical bath subject to centric bottom gas injection. *Metall. Mat. Trans. B* **26,** 241–247.

Iguchi, M., Okita, K., Kasai, N., Nakatani, T., Ueda, H. and Morita, Z. (1996) Bubble and liquid flow behavior agitated by porous nozzle bubbling. *Tetsu-to-Hagane* **82,** 185–190.

Lance, M. and Bataille, J. (1991) Turbulence in the liquid phase of a uniform bubbly air–water flow. *J. Fluid Mech.* **222,** 95–118.

Marie, J. L. and Lance, M. (1983) Turbulence measurements in two-phase bubbly flows using laser Doppler anemometry. *IUTAM Symp. on Measuring Techniques in Gas–Liquid Two-phase Flows*, pp. 141–148.

McDougall, T. J. (1978) Bubble plumes in stratified environments. *J. Fluid Mech.* **85,** 655–672.

Milgram, J. H. (1983) Mean flow in round bubble plumes. *Int. J. Multiphase Flow* **133,** 345–376.

Nihei, Y. and Nadaoka, K. (1995) A study of turbulence modulation in multi-phase flow by numerical simulation. *14th National Symp. on Multiphase Flow*, Matsuyama, Japan, pp. 120–123.

Panchapakesan, N. R. and Lumley, J. L. (1993) Turbulence measurements in axisymmetric jets of air and helium. Part 1. Air jet. *J. Fluid Mech.* **246,** 197–223.

Popper, J., Abuaf, N. and Hetsroni, G. (1974) Velocity measurements in a two-phase turbulent jet. *Int. J. Multiphase Flow* **1,** 715–726.

Reichardt, H. (1943) New theory of free turbulence. *Roy. Aero. Soc. L.* **47,** 167–176.

Sahai, Y. and Pierre, G. R. St. (1992) *Advances in Transport Processes in Metallurgical Systems*. Elsevier, Amsterdam.

Serizawa, A., Kataoka, I. and Michiyoshi, I. (1975a) Turbulence structure of air–water bubbly flow—I. Measuring techniques. *Int. J. Multiphase Flow* **2,** 221–233.

Serizawa, A., Kataoka, I. and Michiyoshi, I. (1975b) Turbulence structure of air–water bubbly flow—II. Local properties. *Int. J. Multiphase Flow* **2,** 235–246.

Serizawa, A., Kataoka, I. and Michiyoshi, I. (1975b) Turbulence structure of air–water bubbly flow—III. Transport properties. *Int. J. Multiphase Flow* **2,** 247–259.

Sheng, Y. Y. and Irons, G. A. (1992) Measurements of the internal structure of gas–liquid plumes. *Metall. Trans. B* **23,** 779–788.

Sun T.-Y. and Faeth G. M. (1986a) Structure of turbulent bubbly jets—I. Methods and centerline properties. *Int. J. Multiphase Flow* **12,** 99–114.

Sun T.-Y. and Faeth G. M. (1986b) Structure of turbulent bubbly jets—II. Phase property profiles. *Int. J. Multiphase Flow*. **12,** 115–126.

Szekely, J., Carlson, G. and Helle, L. (1988) *Ladle Metallurgy*. Springer, Berlin.

Theofanous, T. G. and Sullivan, J. (1982) Turbulence in two-phase dispersed flow. *J. Fluid Mech.* **116,** 343–362.

Tsuji, Y. and Morikawa, Y. (1982) LDV measurements of an air–solid two-phase flow in a horizontal pipe. *J. Fluid Mech.* **120,** 385–409.

Tsuji, Y., Morikawa, Y. and Shiomi, H. (1984) LDV measurements of an air–solid two-phase flow in a vertical pipe. *J. Fluid Mech.* **139,** 417–434.

Tsuji, Y. Tanaka, T. and Yonemura, S. (1994) Particle induced turbulence. *Appl. Mech. Rev.* **47,** 75–79.

Tsuji, Y. (1995) Study of turbulence in multiphase flow—aim at escape from mess. *27th National Symp. on Turbulent Flow*, Osaka, Japan, pp. 9–13.

Wygnanski, I. and Fiedler, H. (1969) Some measurements in the self-reserving jet. *J. Fluid Mech.* **38,** 577–612.

Zuber, N. and Findlay, J. A. (1965) Average volumetric concentration in two-phase systems. *Trans. ASME, J. Heat Transfer* **87,** 453–468.